# Critical science instrument alignment of the James Webb Space Telescope (JWST) Integrated Science Instrument Module (ISIM)

Scott O. Rohrbach[*a], David A. Kubalak[a], Renee M. Gracey[b], Derek S. Sabatke[b], Joseph M. Howard[a], Randal C. Telfer[c], Thomas P. Zielinski[a]

[a]NASA Goddard Space Flight Center, 8800 Greenbelt Rd., Greenbelt, MD 20771

[b]Ball Aerospace and Technologies Corporation, 1600 Commerce St, Boulder, CO 80301

[c]Space Telescope Science Institute, 3700 San Martin Drive, Baltimore, MD 21218

## ABSTRACT

This paper describes the critical instrument alignment terms associated with the six-degree of freedom alignment of each the Science Instrument (SI) in the James Webb Space Telescope (JWST), including focus, pupil shear, pupil clocking, and boresight. We present the test methods used during cryogenic-vacuum tests to directly measure the performance of each parameter, the requirements levied on each, and the impact of any violations of these requirements at the instrument and Observatory level.

**Keywords:** JWST, ISIM, focus, pupil shear, boresight

## 1. INTRODUCTION

The Integrated Science Instrument Module (ISIM) of the James Webb Space Telescope (JWST) is comprised of four Science Instruments (SIs), the Fine Guidance Sensor (FGS), and the ISIM Structure, to which each of the instruments is mounted. The alignment of each instrument prior to delivery was determined with respect to an Ambient Science Instrument Mechanical Interface Fixture (ASMIF), a custom-built platform for each instrument that duplicates the SI mounting interface on the ISIM Structure and provides metrology references that were calibrated with respect to the coordinate system, establishing alignment to the nominal optical interfaces, such as the Optical Telescope Element (OTE) focal surface and exit pupil. Each SI team employed a combination of test and analysis to align and verify the cryogenic alignment of their optical system to the ASMIF-calibrated coordinate system references.

Once each SI was delivered for integration, it was mounted to the ISIM Structure and ambient and cryogenic alignment tests were performed to assess a variety of critical alignment terms, including focus, pupil shear, pupil clocking, field-of-view and boresight.[1] In ISIM Cryogenic Vacuum Tests #2 and #3 (CV2 and CV3, respectively), the performance of each of these terms was measured *in situ*, with appropriate launch-level vibration and acoustic tests performed in between to simulate the magnitude of any shifts in performance due to launch.

## 2. ALIGNMENT ERROR BUDGET DISTRIBUTION

Prior to much of the SI and ASMIF fabrication and assembly, an error budget for the rigid body alignment of each SI was established based on requirements in the ISIM Requirements Document and the allocations to the ISIM and SIs from requirements in the "ISIM to OTE and Spacecraft (IOS) Interface Requirements and Control Document (IRCD)", commonly referred to as the "IOS". Allocations of nine primary requirements covering focus, pupil alignment, boresight alignment and wavefront error (WFE) were distributed among three primary sources of error: 1) ISIM Structure stability and fabrication of the Science Instrument Interface Plates (SIIPs), which act as shim-like custom interfaces between the SI kinematic mount bases and the ISIM Structure, 2) internal alignment errors of each SI, and 3) the uncertainty in placement of the ISIM Structure with respect to the nominal OTE focal surface and exit pupil. Each of the allocations was cast in terms of how much they would impact the 6 degree-of-freedom (6-DOF) alignment of each instrument and assigned a subsystem-level requirement. Finally, these allocations were broken out and assigned to every piece of hardware and metrology tool that affected the alignment of ISIM SIs, including uncertainties in establishing the location of the nominal

[*] Scott.rohrbach@nasa.gov, phone 1 301 286-3197

**ISIM ELEMENT TOP LEVEL PERFORMANCE REQUIREMENTS**

| DOCUMENT | RQMT No | | NC | NS | M | TF | FGS | |
|---|---|---|---|---|---|---|---|---|
| JWST-IRCD-000640 | FROM IOS-IR-5777 | Δf NCP | 1.5 | 1..5 | TBD | 1.5 | 1.5 | mm |
| JWST-IRCD-000640 | IOS-IR-5772 | Δf CP | 1.1 | 1.1 | 1.1 | 1.1 | 1.1 | mm |
| JWST-IRCD-000640 | IOS-IR-5799 (5803 FOR NC) | PUPIL SHEAR | 3.0 | 3.1 | 3.1 | 3.1 | 3.1 | % |
| JWST-RQMT-000835 | FROM ISIM-668/1034/1035 | WFE (ISIM ONLY) | 17 | 17 | 17 | 17 | 17 | nm |
| JWST-IRCD-000640 | IOS-IR-5790 | PUPIL ROLL | 2 | 2 | 2 | 2 | 2 | mr |
| JWST-IRCD-000641 | IOS-IR-5760 | BORE2 | 7.23 | 7.23 | 7.23 | 7.23 | 7.23 | asec |
| JWST-IRCD-000642 | IOS-IR-5760 | BORE3 | 7.23 | 7.23 | 7.23 | 7.23 | 7.23 | asec |

**ERROR BUDGET SOURCE 1**

**ISIM/SI MECHANICAL I/F (SIIP ALIGNMENT)**

| DOCUMENT | RQMT No | REQUIREMENT | | |
|---|---|---|---|---|
| JST-RQMT-002087 | IST-233/234 | SIIP ALIGNMENT | | |
| | | mm dV | amin dR | |
| | | 0.6 | 6 | INTER BIPOD |
| | | 0.43 | 6 | INTRA BIPOD |

**ERROR BUDGET SOURCE 2**

**SI FOCUS AND PUPIL ALIGNMENT TO ISIM/SI MECHANICAL I/F**

| | NC | NS | M | TF | FGS |
|---|---|---|---|---|---|
| Δf (mm) | 0.42 | 0.42 | 0.50 | 0.42 | 0.42 |
| PUPIL SHEAR (%) | 1.00 | 1.00 | 0.50 | 0.50 | 0.50 |
| PUPIL ROLL (mrad) | 1.00 | 1.00 | 1.00 | 1.00 | 1.00 |

| DOCUMENT | RQMT No |
|---|---|
| JWST-IRD-003272 (NIRcam) | NIRcam (FOCUS INCU-1672), (PUPIL INCU-1783) |
| JWST-IRD-000781 (NIRspec) | NIRspec (FOCUS INSU-2138), (PUPIL INSU-2139) |
| JWST-IRD-000782 (MIRI) | MIRI (FOCUS JWST-ICD-000730, 3.1.3.1) |
| JWST-IRD-000782 (MIRI) | MIRI (PUPIL JWST-ICD-000730, 3.1.3.2) |
| JWST-IRD-000783 (FGS) | FGS (FOCUS IF-111), (PUPIL IF-115) |
| JWST-IRD-000783 (FGS) | TF (FOCUS IF-111), (PUPIL IF-115) |
| JWST-IRCD-000640 | PUPIL ROLL (TBD) |

**ERROR BUDGET SOURCE 3**

**COMMON PATH ERROR KNOWLEDGE**

SEE ERROR BUDGET FLOW DOWN

Figure 1. Initial top-level ISIM and IOS requirements associated with 6-DOF alignment of each SI and the ISIM Element as a whole as of 2008. Many allocations have changed since then.

OTE focal surface and exit pupil. Uncertainties are tracked using 2-sigma errors or Student's-t 95% probability limits. The top level requirements and first level allocations are shown in Figure 1. The first two terms, Δf NCP and Δf CP refer to the error in Non-Common Path Focus and the error in Common Path focus, respectively. The magnitudes of many of the requirements have changed since the initial error budget was drafted. In particular, the pupil shear requirement for NIRCam was reduced to 1.8%, the pupil roll requirement for all instruments was increased to 10.6 mrad, and the boresight requirement in each axis for all instruments was increased to 10.2 arcseconds.

## 2.1 Error source 1

ISIM Stability and SIIP alignment errors, are relatively simple in concept. The ISIM Structure is an approximately 2m x 2m x 1.5m bonded composite frame that acts as a metering structure between the FGS and SIs and the OTE and is extremely stiff and stable with respect to how it changes shape when cooled from room temperature to the ~37K operational temperature.[2] The SIIPs (in concept) are 19 simple metal plates that were precision fabricated accounting for the measured ISIM Structure deformations due to cryogenic and gravity effects, and errors in SI alignment. Error Source 1 allocations were separated into terms for the ISIM Structure and the SIIPs, and with each being further sub-allocated to terms for fabrication, metrology, and figure errors due to ambient-to-cryogenic temperature and 1-g-to-0g changes. Since the various errors in fabrication and metrology uncertainties do not result in an unambiguous 6-DOF state of each SI, Monte Carlo simulations are performed using the 2-sigma uncertainties as a bound, yielding 2-sigma uncertainties in the top-level performance parameters of focus, pupil, boresight, and WFE. The same process is used to collect and recast the terms in Error Source 2 and Error Source 3 back into performance parameter values.

Once the ISIM Structure and SIIPs were fabricated and tested, their performance was evaluated through precision metrology and cryo-vacuum tests using photogrammetry to track the location of the instrument mount points down to operational temperatures and representative loads.[2] The result is a single set of error values and uncertainties for the various performance parameters for each instrument, shown in Table 1.

| PERFORMANCE PREDICTION + 2-SIGMA UNCERTAINTY | | | | | | | | |
|---|---|---|---|---|---|---|---|---|
| | NC B | NC A | NS | MIRI | NIRISS | FGS 2 | FGS 1 | |
| Δf | 0.12 | 0.14 | 0.09 | -0.17 | 0.13 | 0.14 | 0.14 | mm |
| PUP2 | -0.46 | -0.46 | -0.29 | 0.42 | -0.27 | -0.27 | -0.27 | % |
| PUP3 | -0.35 | -0.35 | -0.40 | 0.26 | 0.41 | 0.39 | 0.40 | % |
| p roll | 0.58 | 0.59 | 0.56 | 0.71 | 0.62 | 0.63 | 0.63 | mrad |
| bore2 | 0.43 | 0.43 | -0.19 | 0.33 | -0.04 | -0.04 | -0.04 | asec |
| bore3 | 0.28 | 0.34 | 0.57 | 0.22 | 0.28 | 0.37 | 0.46 | asec |

Table 1. Errors plus 2-sigma uncertainties associated with Error Source 1.

## 2.2 Error Source 2

Error Source 2 addresses the performance errors associated with the individual SIs and includes the measurement and 2-sigma uncertainty of their focus offsets, pupil shear, pupil roll, and boresight alignment errors. These terms were allocated to each SI provider, who reported on instrument errors and uncertainties upon delivery. The WFE term from the top level was not sub-allocated to the SIs since it accounts for WFE changes due to changes in 6-DOF alignment of each SI after it

is delivered and installed into the ISIM Structure. The bulk of this paper addresses the other performance parameters associated with instrument alignment.

### 2.3 Error Source 3

The Common Path error portion of the budget defines the allowed error in the 6-DOF alignment between the ISIM and the nominal OTE focal surface. This error source comprises a combination of errors from ambient temperature measurements, component and assembly cryogenic tests, and a series of cryo-vacuum OSIM calibration tests. The results of these test were used to determine the optimum alignment between the ISIM and OTE references for maximum SI performance. The majority of the Common Path Error is uncertainty in the determination of optimum alignment and includes the uncertainties in the location of the ISIM Test Platform (ITP), the Master Alignment Target Fixture (MATF), the OTE Simulator (OSIM[3]) light stimulus, OSIM-to-MATF knowledge, photogrammetry, data analysis of best focus and pupil position, and the ability to accurately adjust the ISIM kinematic struts in the event that a common path adjustment is needed once all of the instruments are installed and aligned. The individual components in each subsystem were considered, with allocations assigned to each piece of hardware or measurement that could impact our knowledge of the ISIM vs nominal OTE references. The MATF is the primary alignment reference that relates the OSIM and ISIM subsystems to the nominal OTE focal surface.

While the original error budget provided allocations to hundreds of component terms, the resulting errors and uncertainties are contained entirely by the calibration report for OSIM and the location of the focal surface, chief ray angles and boresight errors it achieves.

## 3. PRIMARY ISIM ALIGNMENT REQUIREMENTS

As noted in Figure 1, there are six primary performance parameters associated with the 6-DOF alignment of each SI and the ISIM Element as a whole. These parameters and the associated requirements are:

1. Common path focus: IOS-IR-5772 The on-orbit focus errors relative to the Optomechanical Reference Plane A and the nominal OTE focal surface, caused by the ISIM Element shall not exceed +/- 1.1 mm along the JWST instrument boresight chief rays.

2. Non-common path focus: IOS-IR-5777 Excluding the MIRI, the ISIM Element shall leave at least +/-1.60 mm of instrument focus adjustment range along the JWST instrument boresight chief rays in the OTE image space after ISIM focus errors have been corrected.

3. Pupil shear: IOS-IR-5799 Excluding the NIRCam channel, the on-orbit, instrument pupil shear error with respect to the A Reference caused by the ISIM Element shall not exceed 3.1%. (i.e., FGS, MIRI, NIRISS, NIRSpec)

   IOS-IR-5798 On-orbit, after articulation of the NIRCam pupil adjustment mechanism, the pupil shear error in the Module A and B NIRCam channel with respect to the Optomechanical Reference Plane A, due to the ISIM Element shall not exceed 1.8%.

4. Wavefront Error: ISIM-668 The system WFE introduced by the ISIM Structure shall be less than the values in Table 3-13. (For NIRCam, NIRSpec, FGS-Guider, and NIRISS Total = 22 nm RMS, Low = 22 nm, Mid = 4 nm, High = 0 nm; For MIRI Total = 71 nm RMS, Low = 71 nm, Mid = 8 nm, High = 0 nm)
   Note: The definitions of Low, Mid, and High spatial frequency WFE are as follows:
   Low spatial frequency WFE: spatial frequency </= 5 cycles/aperture
   Mid spatial frequency WFE: 5 cycles/aperture < spatial frequency </= 30 cycles/aperture
   High spatial frequency WFE: spatial frequency > 30 cycles/aperture.

   ISIM-1034 The maximum allowable change in the WFE induced by the ISIM Structure, and the breakdown of the maximum allowable WFE by spatial frequency range shall be as shown in Table 3-15 for a temperature change of 0.25K. (Total = 8 nm RMS, Low = 8 nm, Mid = 0 nm, High = 0 nm)

   ISIM-1035 The maximum allowable change in the WFE induced by the ISIM Structure, and the breakdown of

the maximum allowable WFE by spatial frequency range shall be as shown in Table 3-15 for a temperature change of 0.5K. (Total = 8 nm RMS, Low = 8 nm, Mid = 0 nm, High = 0 nm)

5. Pupil roll: IOS-IR-5790 The ISIM Element shall align each SI and the FGS-Guider to the nominal OTE exit pupil in the on-orbit environment such that the pupil clocking of each instrument does not exceed ± 10.6mr about its respective central chief ray.
6. Boresight: IOS-IR-5706 Relative to the nominal OTE to ISIM interface, the ISIM Element boresight errors relative to the nominal design boresight angles in the NIRCam, NIRSpec, MIRI and FGS-Guider and NIRISS channels as specified in Table 5-9 shall not exceed 0.17 arc minutes per axis in the on-orbit environment for the nominal OTE design.

Structural/Thermal/Optical (STOP) modeling of the impact of ISIM Structure deformations on the mid and high-frequency WFE are insignificant. The low frequency term is completely dominated by the power term associated with a bulk shift of ISIM in the V1 direction, i.e., focus. Since the uncertainty in focus is already a term in the larger WFE budget for each instrument, that term is no longer separately tracked here.

### 3.1 Common Path Focus

The "$0^{th}$ order" placement of the ISIM Element with respect to the OTE is constrained more by the range over which the OTE focal surface can be adjusted than by the depth-of-field or range of the focus adjustment mechanisms. The Secondary Mirror (SM) of the OTE can be adjusted along the Master Chief Ray (MCR) in order to move the focal surface over a range of ±1.1 mm with respect to its nominal location. This adjustment capability allows the entire ISIM Element a small placement error along the MCR. As such, the IOS-IR-5772 requirement in the IOS reads, "The on-orbit focus errors relative to the Optomechanical Reference Plane A and the nominal OTE focal surface, caused by the ISIM Element shall not exceed ± 1.1 mm along the JWST instrument boresight chief rays."

Since MIRI has a depth of focus larger than ±1.1 mm, and the other SIs have focus mechanisms with sufficient range to accommodate any ISIM Element position within the requirement, IOS-IR-5772 can be satisfied entirely by the knowledge uncertainty budget for the ISIM Element. Three top-level uncertainty terms dominate the budget:

1. Uncertainty in the location of the OSIM focal surface with respect to the nominal OTE focal surface. The position the OSIM focal surface was calibrated in a series of cryo-vacuum tests using a science instrument surrogate called the Beam Image Analyzer (BIA). The location of the BIA with respect to OSIM and the MATF was primarily determined by photogrammetry and the internal Advanced Displacement Metrology (ADM) system. The location of the OSIM focal surface was calibrated with respect to the nominal OTE focal surface to within ±0.15 mm 2-sigma along the V1 axis.
2. Uncertainty in determining best focus of each SI by sweeping the location of the OSIM focus through a ±5 mm range across a variety of locations in each SI field.
3. Uncertainty in placement of new detector surfaces with respect to the old detector surfaces measured in CV2 when new detectors were installed between CV2 and CV3. (This accounts for the fact that any small shift seen in environmental testing between CV2 and CV3 may be due to either hardware shifts or due to the metrology uncertainty during detector replacement.)

| | | | | | | | | | | | |
|---|---|---|---|---|---|---|---|---|---|---|---|
| | | | | ISIM Requirement | 1.10 | | | | | | mm |
| | | | | | | | | | | | |
| | | | | Margin vs Requirement | 0.76 | 0.48 | 0.86 | 0.74 | 0.84 | 0.92 | |
| | | | | | 69.3 | 43.5 | 78.6 | 67.1 | 76.6 | 83.3 | % |
| | | | | | NIRSpec | MIRI | NIRISS | FGS | NCA | NCB | |
| **Total Bottoms-up Estimate** | | | | | **0.34** | **0.62** | **0.24** | **0.36** | **0.26** | **0.18** | |
| | Common Path | | | | | | | | | | |
| | | MIRI focus offset | | | | 0.38 | | | | | |
| | | | | | | | | | | | |
| | Uncertainties (RSS of terms below) | | | | 0.34 | 0.24 | 0.24 | 0.36 | 0.26 | 0.18 | |
| | | Focus determination uncertainty | | | 0.28 | 0.18 | 0.10 | 0.09 | 0.10 | 0.10 | |
| | | | | | | | | | | | |
| | | CV2-to-CV3 shift and FPA swap metrology uncertainty | | | 0.114 | 0.072 | 0.15 | 0.32 | 0.18 | 0.03 | |
| | | | | | | | | | | | |
| | | OSIM alignment uncertainty | | | 0.15 | 0.15 | 0.15 | 0.15 | 0.15 | 0.15 | |

Table 2. Error budget for the IOS-IR-5772 requirement for Common Path Focus showing compliance for all instruments.

The final error budget, including a term for absolute MIRI defocus since it does not have a focus mechanism to compensate for ISIM Element misplacement, is shown in Table 2. The requirement is met for all instruments.

### 3.2 Non-Common Path Focus

As noted above, the Non-Common Path focus requirement dictates that each instrument with a focus mechanism have enough range to adjust their best focus position more than ±1.6 mm in the OTE focal surface space (abbreviated as "±1.6 mm OTE" or "OTE space" to refer to the OTE focal space units in general). Since each instrument has its own magnification, there is not a 1:1 correspondence between the range of the mechanisms themselves and the range in OTE space. The ranges reported here are stated in terms of OTE space, not local mechanism space.

The budget for this requirement starts with the available range when the mechanism is at its center position (i.e., half of the total available travel range), and subtracts off the distance from center the mechanism is at as of the end of ISIM CV3. The uncertainties in a variety of terms must also be subtracted which are:

1. Errors in determining best focus,
2. Uncertainties in shifts from the ground condition to on-orbit operation (STOP analysis)[4],
3. Changes through environmental testing and metrology uncertainties during the detector replacement process,
4. Uncertainty of the OSIM focal surface vs the nominal OTE focal surface[3], and
5. Focus mechanism resolution in OTE space

Terms 2 and 4 are described elsewhere. Terms 3 and 5 were reported via internal deliverables. Determining best focus, and the errors associated with that are described below. The error budget associated with this requirement is shown for each instrument with a focus mechanism in Table 3.

| | | | | | | | | | | | | |
|---|---|---|---|---|---|---|---|---|---|---|---|---|
| | | | | ISIM Requirement | 1.60 | | | | | | | mm |
| | | | | Margin vs Requirement | 8.96 | | 2.97 | 9.49 | 8.93 | 10.01 | | |
| | | | | | NIRSpec | | NIRISS | FGS | NIRCam A | NIRCam B | | |
| **Total Bottoms-up Range remaining (Magnitude - Uncertainty)** | | | | | **10.56** | | **4.57** | **11.09** | **10.53** | **11.61** | | |
| **Magnitude (best estimate of remaining range)** | | | | | **10.89** | | **4.93** | **11.32** | **10.78** | **11.79** | | |
| 1 | Total mechanism range (from center) | | | | 10.90 | | 5.27 | 14.50 | 12.69 | 12.69 | | |
| 3 | CV3 on-orbit focus position w.r.t. center of travel | | | | 0.01 | | 0.34 | 3.18 | -1.91 | -0.90 | | |
| | | after adjustment to on-orbit position at end of test | | | | | | | | | | |
| **Uncertainty (RSS of all terms below)** | | | | | **0.33** | | **0.36** | **0.23** | **0.26** | **0.18** | | |
| 5 | CV3 on-orbit uncertainties | | | | 0.28 | | 0.10 | 0.09 | 0.10 | 0.10 | | |
| 4 | CV2-to-CV3 shifts and FPA swap metrology uncertainty | | | | 0.056 | 0.072 | 0.32 | 0.15 | 0.18 | 0.03 | | |
| 2 | OSIM focal location uncertainty | | | | 0.15 | | 0.15 | 0.15 | 0.15 | 0.15 | | |
| 8 | Mechanism positioning uncertainty | | | | 0.05 | | 0.002 | 0.002 | 0.02 | 0.02 | | |

Table 3. Error budget for IOS-IR-5772, Non-Common Path focus showing compliance for all instruments. NIRISS has the smallest margin of available travel, but it is still 186% of the requirement.

Best focus at any field point is determined by scanning the OSIM focal surface through a range positions and fitting the images to one of a variety of focus metrics. Based on analysis of simulated data we have identified optimal metrics for each instrument, i.e. metrics that exhibit small errors in Monte Carlo simulations and not strongly affected by aberration content. The choice is mostly dependent on the sampling ratio for focus test (Q=wavelength x f-number / pixel pitch).

- Guider (Q=0.92): 3x3 ensquared energy (the fraction of total light in a 3x3 pixel region where the peak pixel is the center of the 3x3 box)
- NIRISS (Q=0.74): 3x3 ensquared energy
- MIRI (Q=1.56): Encircled energy at first dark Airy ring (R=1.9 pixels)
- NIRCam Short Wavelength (SW) channel (Q=2.13): Encircled energy at first dark Airy ring (R=2.6 pixels)
- NIRCam Long Wavelength (LW) channel (Q=1.59): Encircled energy at first dark Airy ring (R=1.9 pixels)
- NIRSpec (Q=0.47): Gaussian FWHM, 2x2 ensquared energy

These metrics are either the same as used by SI teams or have been shown to correlate well with the SI team results through CV2 and CV3. An example focus sweep is shown in Figure 2 for the center field point in NIRISS from -5.3 to +3.0 mm OTE. (Multiple images are taken at each defocus value to improve statistics.)

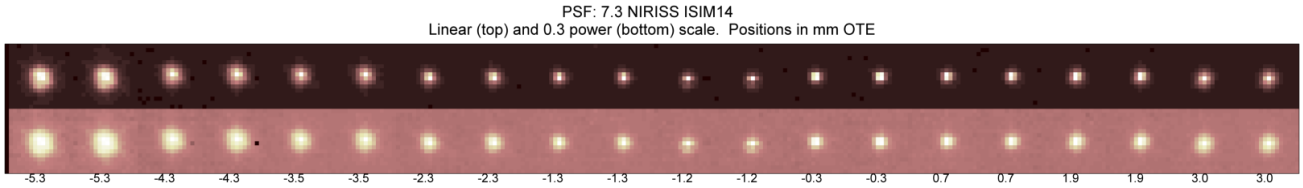


Figure 2. Example focus sweep used to determine best focus at the center field point in NIRISS. The top row is a linear stretch, while the bottom row are the same images using a log stretch.

For each instrument, the focus metric is plotted and fit to a Gaussian curve, examples of which is shown in Figure 3.

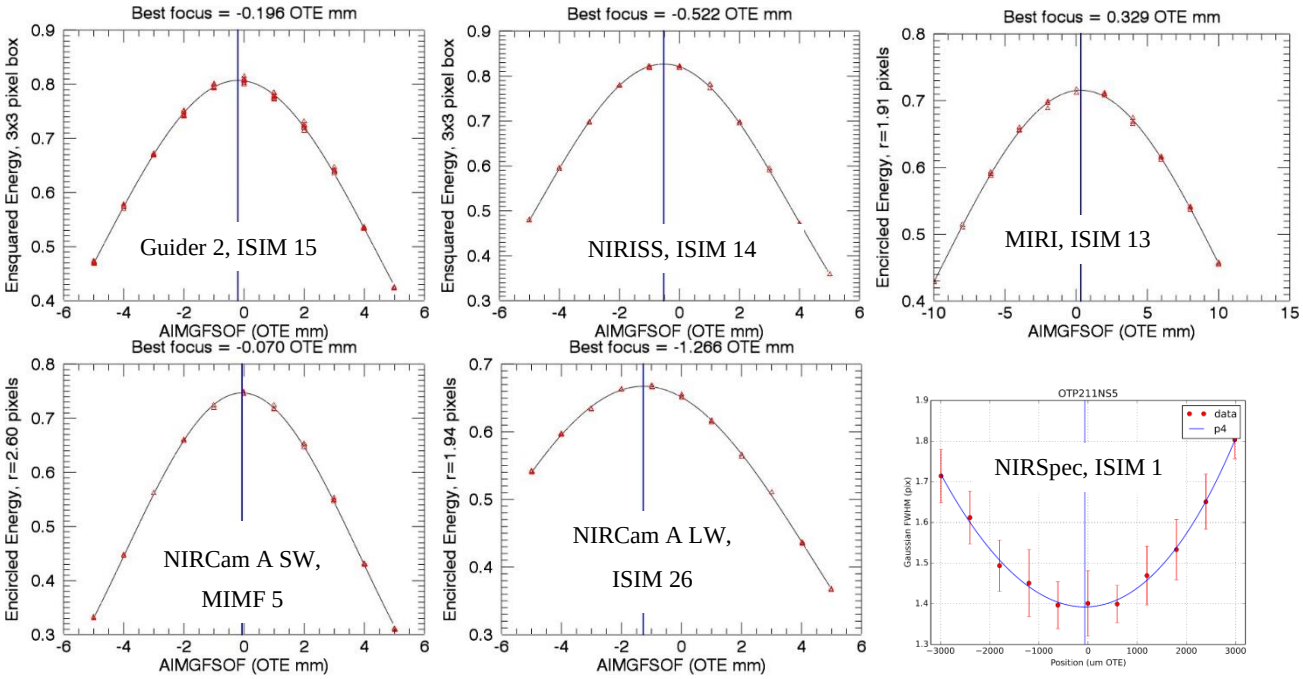


Figure 3. Focus metrics and fits of focus sweeps at the center-most field point in each SI.

Once the best focus at each field point is determined using the above metrics, then the best focus over the entire field needs to be set. Weighting of is done differently for each instrument since they each have their own functional needs. The various weighting metrics are:

- NIRISS – Fit a surface to data and minimize average FWHM over field.
- NIRSpec – Minimize Gaussian FWHM at the ISIM 1 field point (center of the S1600A fixed slit).
- NIRCam – Maximize WFE margin to requirement for worst of measured field points, considering filters F200W (SW); F250M, F323N, and F466N (LW).
- Guider – Maximize weighted sum of ensquared energy for measured field points. Weighting shown in Figure 4.

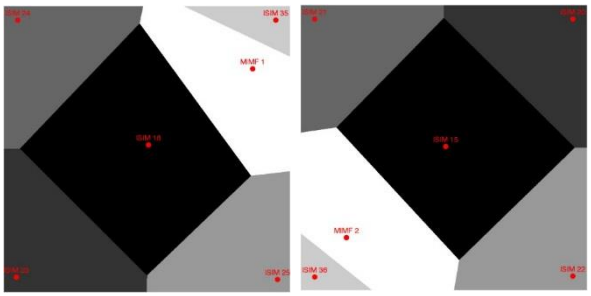

| Field Point | Weight |
|---|---|
| ISIM 16 | 0.334 |
| ISIM 23 | 0.170 |
| ISIM 24 | 0.142 |
| ISIM 25 | 0.142 |
| ISIM 35 | 0.084 |
| MIMF 1 | 0.127 |
| ISIM 15 | 0.352 |
| ISIM 20 | 0.146 |
| ISIM 21 | 0.144 |
| ISIM 22 | 0.144 |
| ISIM 36 | 0.025 |
| MIMF 2 | 0.189 |

Figure 4. Weighting scheme for the Guider channels. The border of each region is equidistant from the nearest measured field points.

Once best focus over field is calculated for each instrument, the focus mechanism is set and the residual defocus at each field point can be calculated for comparison to the power term derived from a phase retrieval measurement of wavefront error[5]. The residual defocus for each field point from the ISIM CV2 and CV3 tests is shown in Figure 5.

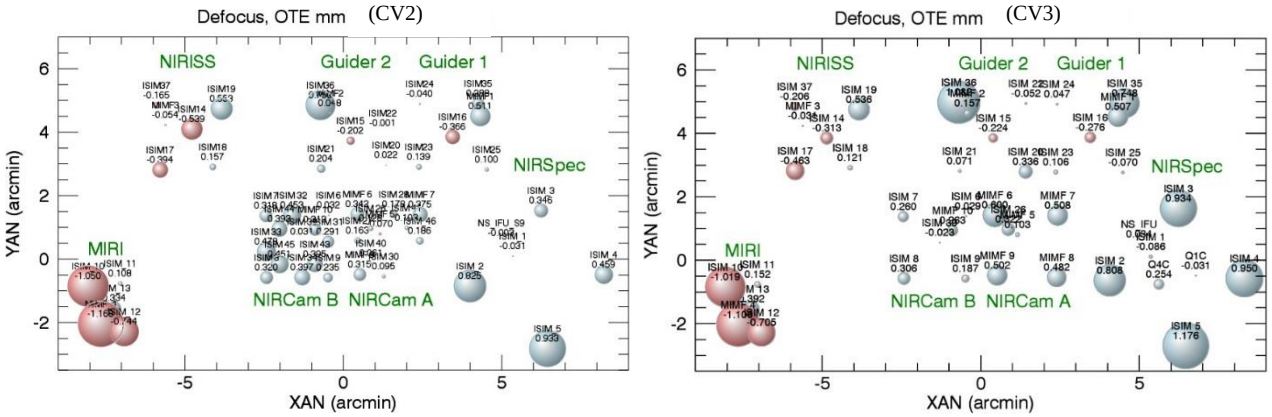


Figure 5. Residual defocus for each field point measured in ISIM CV2 and CV3. The size of each bubble corresponds to the magnitude of the defocus. Blue bubbles are positive defocus and red bubbles are negative.

Finally, for NIRCam, best focus is also varies over wavelength since NIRCam has refractive elements in its optical design. Focus sweeps were performed at the centermost SW field point in both NIRCam modules for a variety of wavelengths. The residual defocus in NIRCam A is plotted in Figure 6 along with the modeled residual defocus vs wavelength at that field point. There is some deviation from the model in the LW channels, primarily due to curvature in some LW filters as a result of coating stress causing a slight shortening of the optical path. These deviations from the model are accounted for in the wavefront error budget for NIRCam.

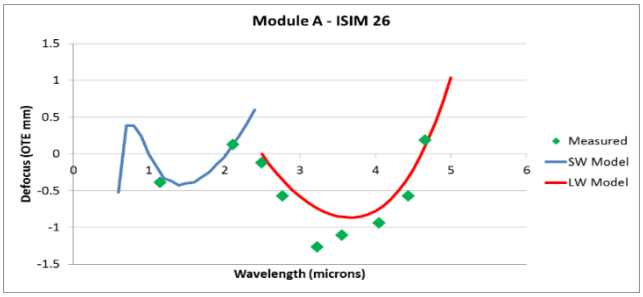


Figure 6. Modeled and observed residual defocus vs wavelength at the centermost field point measured in NIRCam A.

### 3.3 Pupil shear

In the integrated observatory, the OTE exit pupil and SI entrance pupils are nominally coincident at a location just downstream from the Fine Steering Mirror (FSM). The SI entrance pupils are somewhat oversized with respect to the OTE exit pupil in order to avoid vignetting for small misalignments of the SIs with respect to the OTE. The SI pupils cannot be too large, however, since there would otherwise be a stray light path that allows a direct sky view into the instruments (a "rogue path"). Therefore, pupil stops that are large enough to account for small misalignments and pupil wander and small enough to block stray light paths were required and implemented. The pupil shear budget was distributed from the Observatory level such that each SI is allowed up to 3.1% pupil shear where shear is defined as the radial distance the pupil is displaced divided by the diameter of the OTE exit pupil (approximately 152 mm). There is a magnification term that comes into play if the SI entrance pupil is not located at the same point along the optical

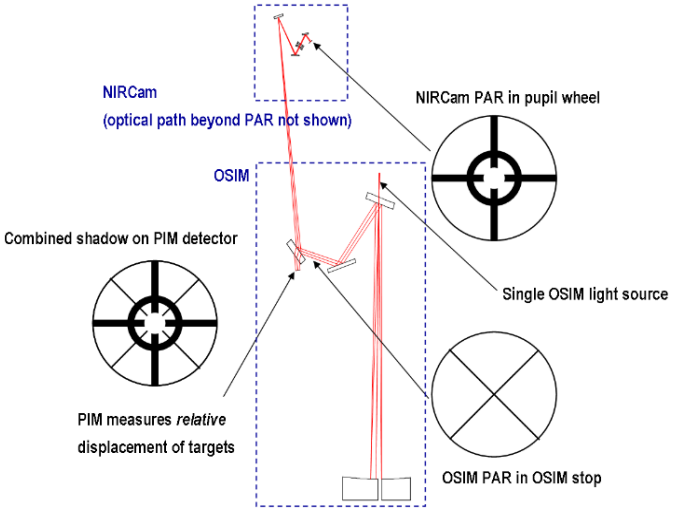


Figure 7. Pupil imaging using the OSIM and SI PARs

path as the FSM mask (the functional pupil stop of the OTE, even though the pupil plane is not technically located at that plane). If the SI entrance pupil is downstream of the FSM mask, then the apparent SI stop at the FSM mask becomes larger, increasing the risk of the rogue path being opened. If the SI entrance pupil is upstream of the FSM mask, then the apparent SI stop becomes smaller, increasing the risk of vignetting light from the OTE.[6]

Pupil shear is measured *in-situ* using a combination of two Pupil Alignment References (PARs) and the Pupil Imaging Module (PIM) assembly within OSIM.[7] Light from the OSIM Source Delivery Module (SDM) passes through one of two OSIM PARs (either the "crossed ladder" mask or a simple cross-hair mask shown in Figure 7.) to the SI being tested where it reflects back from a PAR at the SI pupil. The reflected light comes back into OSIM and some fraction passes through the 3rd fold mirror and is captured by the PIM.

FGS

The FGS PAR is a surface that is machined into the center of the third mirror in the FGS three mirror assembly (TMA), shown in Figure 8. PIM images of the FGS PAR and OSIM PAR1 from CV2 and CV3 are overlaid in yellow and green in Figure 9, showing very little change from CV2 to CV3.

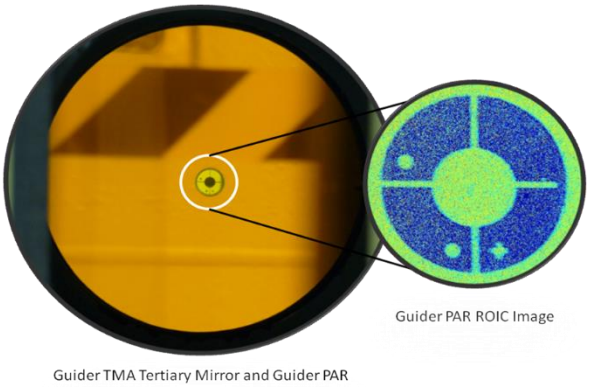


Figure 8. FGS PAR and reflected image from instrument-level testing.

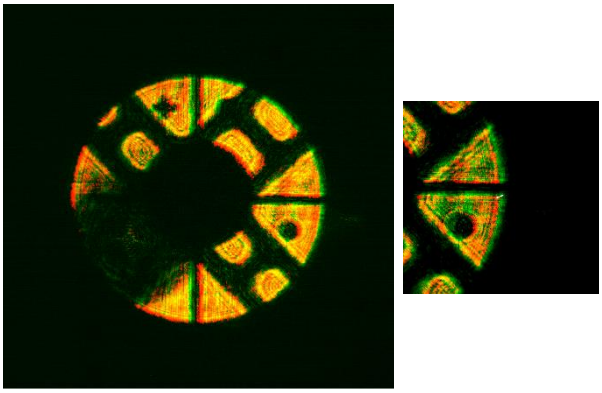

Figure 9. OSIM PIM images of the OSIM PAR1 and the FGS PAR from ISIM CV2 and CV3.

NIRISS

The NIRISS PAR is located in the center of the CLEARP pupil wheel element, shown in Figure 10. The OSIM PIM image is shown in Figure 11. The NIRISS PAR is significantly larger in OSIM pupil space than the FGS PAR, so more of the OSIM PAR1 is visible than in the FGS PIM image. One can see a clear offset between the NIRISS PAR and the ladder legs of the OSIM PAR1. Some of this is due to a known and calibrated shift between the center of the NIRISS pupil and the center of the PAR. But, there is also nearly a 2% shear in the horizontal direction after all of the OSIM and NIRISS integration alignment errors are accounted for.

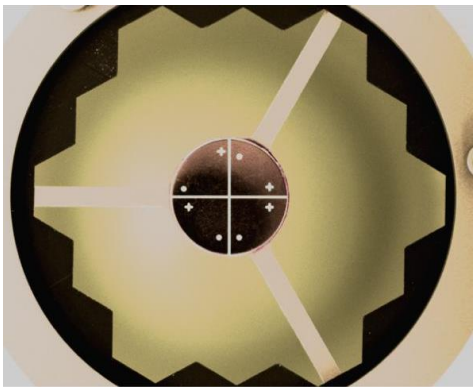

Figure 10. NIRISS CLEARP pupil wheel element with the PAR at the center.

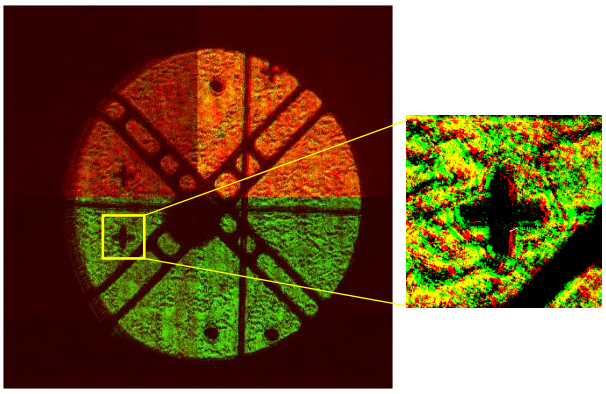

Figure 11. OSIM PIM images of the OSIM PAR1 and the NIRISS PAR from ISIM CV2 and CV3.

MIRI

The MIRI PAR is located on an opaque element in the MIRI Filter Wheel. A mechanical drawing of the MIRI PAR is shown in Figure 12, and CV2 and CV3 PIM images are shown in Figure 13, demonstrating excellent stability through environmental testing between CV tests. Like the NIRISS PAR, the MIRI PAR has a large known offset with respect to the center of the MIRI Alignment Lens element, which defines the center of the MIRI pupil. This offset is accounted for in the evaluation of pupil shear.

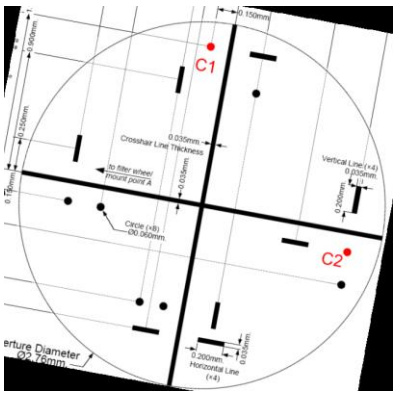


Figure 12. Drawing of the MIRI PAR. The small fiducials do not show up well in OSIM PIM images.

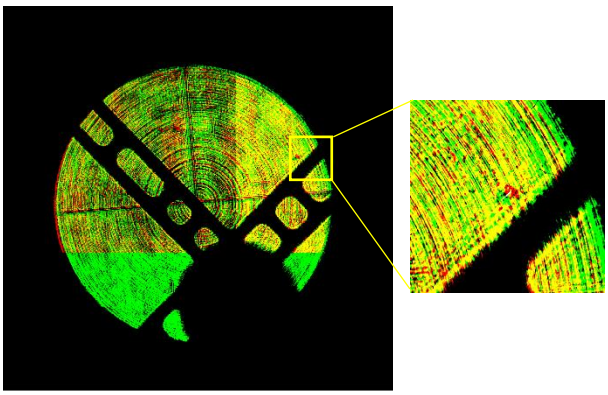

Figure 13. OSIM PIM image of the OSIM PAR1 and MIRI PAR from ISIM CV2 and CV3.

NIRSpec

The NIRSpec PAR is also located on an opaque filter wheel element. A drawing of the NIRSpec PAR is shown in Figure 14 and the PAR fiducial markings can be seen in the OSIM PIM image shown in Figure 15. A shift between the CV2 and CV3 shears is visible in the zoomed portion of the image. It is impossible to separate the impacts of deintegration/reintegration of the instrument to replace the Focal Plane Assembly and shifts due to environmental testing between CV tests, so the entire observed shift plus metrology uncertainty needs to be carried as an uncertainty in the ground-to-orbit pupil shear budget.

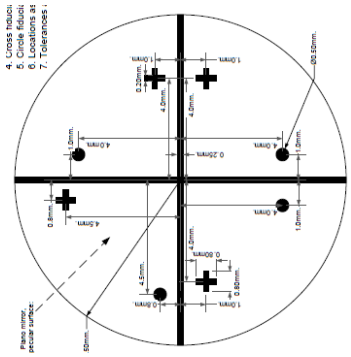

Figure 14. Drawing of the NIRSpec PAR.

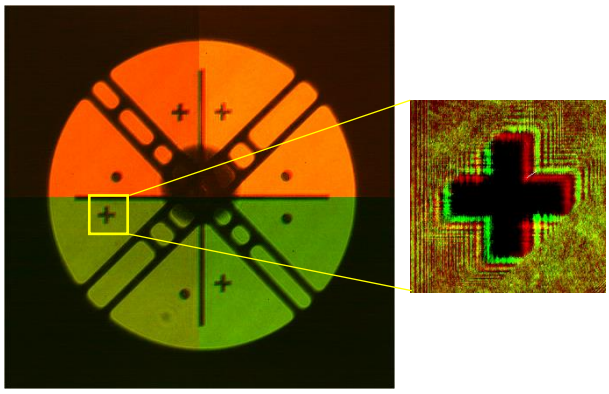

Figure 15. OSIM PIM image of the OSIM PAR1 and NIRSpec PAR from ISIM CV2 and CV3.

NIRCam

The NIRCam PARs are located on the PINHOLE short wavelength pupil wheel elements. A CAD image of the Module A PAR is shown in Figure 16. These elements contain not only the PAR fiducials, but also small fiducial holes through which internal lamps emit light going both outward and inward toward the detectors. Due to a mis-ordering during fabrication the reflective elements were machined after being polished, resulting in a distorted return in the OSIM PIM, shown in Figure 17. As such, it is very difficult to determine pupil shear accurately using these images.

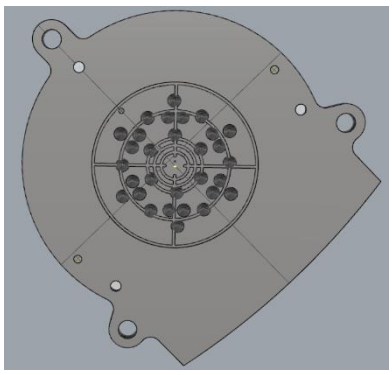

Figure 16. CAD image of the NIRCam A PINHOLE element with the PAR fiducials at the center.

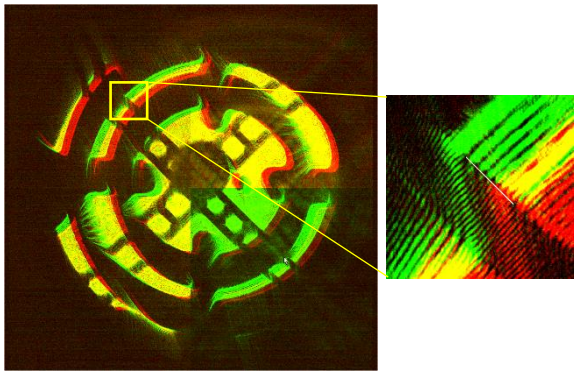

Figure 17. OSIM PIM images of the OSIM PAR1 and the NIRCam A PAR.

Fortunately, NIRCam was designed with a Pupil Imaging Lens (PIL) module that can be inserted in the SW path after the Camera triplet lens assembly in order to view the pupil plane illumination using the NIRCam SW detector. The PIL was originally included to provide on-orbit alignment of the NIRCam entrance pupil with respect to the OTE exit pupil. The imaging apertures in NIRCam are highly oversized and cannot be fully illuminated with any of the OSIM pupil elements, so the assessment of pupil alignment in ISIM CV2 and CV3 was performed by viewing the alignment of the OSIM Tricontagon pupil with respect to the NIRCam Dispersed Hartmann Sensor (DHS) elements with the PILs.

A representative PIL image of the OSIM Tricontagon and the NIRCam CLEAR element is shown as a reference in Figure 18. The NIRCam pupil wheel is then rotated to insert the DHS, in Figure 19. The Tricontagon struts that represent the Secondary Mirror Support System arms are visible to provide a clear reference, and the apertures in the DHS pupil provide a simple measure of the pupil shear for the DHS element. The DHS is visibly clocked in the pupil plane. This will be addressed later in Section 3.4, Pupil roll.

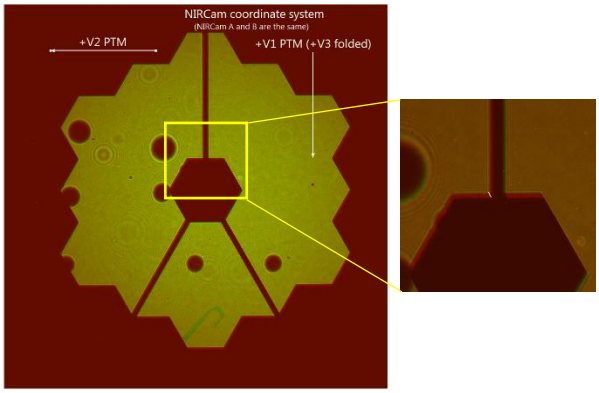


Figure 18. PIL Images of the OSIM Tricontagon from ISIM CV2 and CV3.

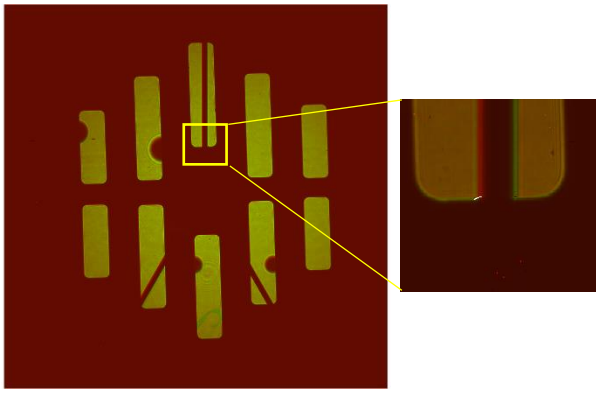

Figure 19. PIL Images of the OSIM Tricontagon and NIRCam A DHS from ISIM CV2 and CV3.

The measured pupil shear, accounting for all calibration shifts and uncertainties, is shown in Table 4 for all instruments at the end of CV2, the beginning of CV3 (to demonstrate deintegration/reintegration shifts and environmental testing effects), and the end of CV3 once all mechanisms were adjusted to the on-orbit condition.

| CV2 FOB results | Shear | | | | Uncertainties | | | |
|---|---|---|---|---|---|---|---|---|
| | V2 (%) | V3 (%) | Rad (%) | Roll (mR) | V2 (%) | V3 (%) | Rad (%) | Roll (mR) |
| Requirement | -- | -- | 3.10 | 10.60 | -- | -- | 3.10 | 10.60 |
| FGS Guider | -0.49 | 0.89 | 1.01 | -10.23 | 0.29 | 0.29 | 0.42 | 10.19 |
| FGS NIRISS | 0.54 | -0.38 | 0.66 | -7.36 | 0.31 | 0.29 | 0.42 | 10.47 |
| MIRI | -0.87 | 0.99 | 1.32 | 2.27 | 0.31 | 0.32 | 0.44 | 10.39 |
| NIRSpec | 0.35 | 0.25 | 0.43 | -21.11 | 0.30 | 0.30 | 0.42 | 10.99 |
| NIRCam A (PAR) | 0.81 | -2.59 | 2.72 | 14.81 | 0.30 | 0.30 | 0.42 | 8.33 |
| NIRCam A (PIL) | 0.41 | -0.52 | 0.67 | -30.20 | 0.28 | 0.28 | 0.39 | 10.08 |
| NIRCam B (PAR) | -0.68 | -2.83 | 2.91 | -25.46 | 0.30 | 0.30 | 0.42 | 8.30 |
| NIRCam B (PIL) | 0.08 | -0.53 | 0.54 | 33.55 | 0.28 | 0.28 | 0.39 | 10.08 |

| CV3 IOB results | Shear | | | | Uncertainties | | 1σ | |
|---|---|---|---|---|---|---|---|---|
| | V2 (%) | V3 (%) | Rad (%) | Roll (mR) | V2 (%) | V3 (%) | Rad (%) | Roll (mR) |
| Requirement | -- | -- | 3.10 | 10.60 | -- | -- | 3.10 | 10.60 |
| FGS Guider | -0.59 | 0.73 | 0.94 | -18.88 | 0.29 | 0.29 | 0.42 | 10.19 |
| FGS NIRISS | 0.63 | -0.27 | 0.68 | -7.37 | 0.31 | 0.29 | 0.42 | 10.47 |
| MIRI | -0.99 | 0.83 | 1.29 | -6.48 | 0.31 | 0.32 | 0.44 | 10.39 |
| NIRSpec | 0.17 | 0.09 | 0.19 | -21.14 | 0.30 | 0.30 | 0.42 | 10.99 |
| NIRCam A (PAR) | 0.49 | -2.00 | 2.06 | -7.90 | 0.30 | 0.30 | 0.42 | 8.33 |
| NIRCam A (PIL) | 0.21 | 0.29 | 0.36 | -30.93 | 0.28 | 0.28 | 0.39 | 10.08 |
| NIRCam B (PAR) | -0.80 | -2.52 | 2.65 | -25.45 | 0.30 | 0.30 | 0.42 | 8.30 |
| NIRCam B (PIL) | -0.06 | 0.12 | 0.13 | 33.59 | 0.28 | 0.28 | 0.39 | 10.08 |

| CV3 FOP results | Shear | | | | Uncertainties | | 1σ | |
|---|---|---|---|---|---|---|---|---|
| | V2 (%) | V3 (%) | Rad (%) | Roll (mR) | V2 (%) | V3 (%) | Rad (%) | Roll (mR) |
| Requirement | -- | -- | 3.10 | 10.60 | -- | -- | 3.10 | 10.60 |
| FGS Guider | -0.54 | 0.72 | 0.90 | -27.62 | 0.29 | 0.29 | 0.42 | 10.19 |
| FGS NIRISS | 1.51 | -0.41 | 1.56 | -2.95 | 0.31 | 0.29 | 0.42 | 10.47 |
| MIRI | -1.00 | 0.78 | 1.27 | -10.78 | 0.31 | 0.32 | 0.44 | 10.39 |
| NIRSpec | 0.21 | 0.06 | 0.22 | -16.77 | 0.30 | 0.30 | 0.42 | 10.99 |
| NIRCam A (PAR) | 0.20 | -2.04 | 2.05 | 18.32 | 0.30 | 0.30 | 0.42 | 8.33 |
| NIRCam A (PIL) | -0.11 | 0.08 | 0.13 | -30.93 | 0.28 | 0.28 | 0.39 | 10.08 |
| NIRCam B (PAR) | -1.01 | -2.35 | 2.55 | -42.91 | 0.30 | 0.30 | 0.42 | 8.30 |
| NIRCam B (PIL) | 0.00 | 0.00 | 0.00 | 33.59 | 0.28 | 0.28 | 0.39 | 10.08 |

Table 4. Pupil shear and roll (clocking) for each instrument as of the end of ISIM CV2 (Final Optical Baseline), the beginning of ISIM CV3 (Initial Optical Baseline) and the end of ISIM CV3 (Final Optical Performance).

Pupil shear measurement through the entire ISIM cryo-vacuum test campaign are plotted in Figure 20. The lines for each instrument indicate the history of each instrument's shear and the small circles represent the RMS uncertainty in the shear measurement itself. Most are relatively stable except for NIRISS. This is due to the fact that the NIRISS focus mechanism is the pickoff mirror, and moving the mirror in focus also shears the pupil in a predetermined fashion. Unlike NIRCam, the focus mechanism does not have an additional tip/tilt adjustment to actively align the pupil. So, any time the focus of the instrument is adjusted the pupil shear also changes accordingly. When the other ISIM-level uncertainties are included the total NIRISS shear plus 2-σ uncertainty approaches the ≤ 3.1% shear requirement. Fortunately, the tangential direction of the NIRISS wheels at the pupil position is in the V2 direction (the horizontal axis in this plot), so a change in the flight software is being implemented that will change the V2 shear by -0.8%, providing significant margin against the requirement. The NIRCam PAR values are provided only for reference and to show that the pupil is stable over time.

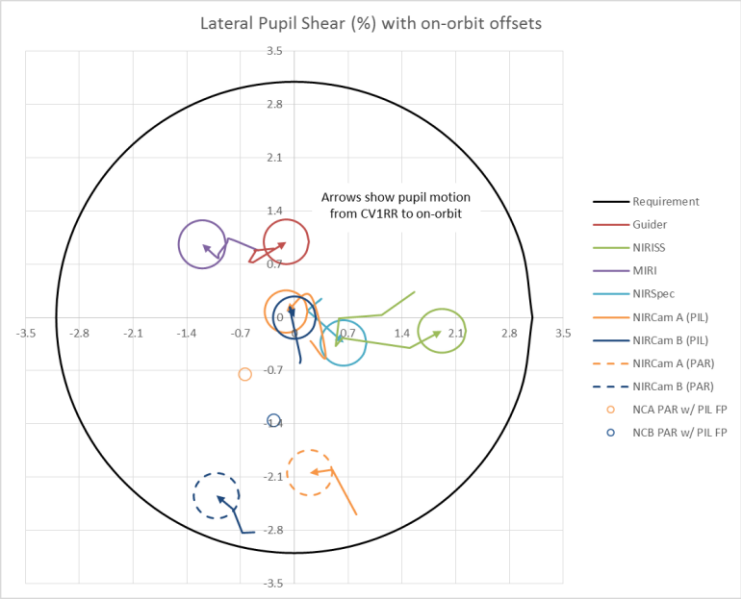


Figure 20. Pupil shear history for all instruments over the ISIM CV campaign. The large black circle is the 3.1% requirement limit. The smaller circles are the 1-σ uncertainty in the shear measurement.

The complete error budget, including the measurements above and the other ISIM-level uncertainties is shown in Table 5.

| | | | | ISIM Requirement | 3.10 | | | | 1.80 | | % |
|---|---|---|---|---|---|---|---|---|---|---|---|
| | | | | Margin vs Requirement | 1.47 | 0.62 | 0.28 | 1.24 | 0.50 | 0.75 | |
| | | | | | NIRSpec | MIRI | NIRISS | FGS | NIRCam A | NIRCam B | |
| **Total Bottoms-up Estimate (Magnitude + Uncertainty)** | | | | | **1.63** | **2.48** | **2.82** | **1.86** | **1.30** | **1.05** | |
| **Magnitude (best estimate of radial shear)** | | | | | **0.72** | **1.54** | **1.93** | **1.00** | **0.14** | **0.00** | |
| | Non-Common Path | | | | | | | | | | |
| 1 | | Radial shear (adjusted to on-orbit) | | | 0.72 | 1.54 | 1.93 | 1.00 | 0.14 | 0.00 | |
| **Uncertainty (RSS of all terms below)** | | | | | **0.90** | **0.95** | **0.89** | **0.85** | **1.17** | **1.05** | |
| 3 | | CV3 uncertainties | | | 0.85 | 0.88 | 0.85 | 0.83 | 0.78 | 0.78 | |
| 4 | | CV2-to-CV3 changes | | | 0.23 | 0.19 | 0.26 | 0.18 | 0.83 | 0.66 | |
| 19 | | Wheel repeatability | | | 0.20 | 0.28 | | | 0.25 | 0.25 | |

Table 5. ISIM pupil shear error budget showing compliance with the requirements IOS-IR-5798 (NIRCam pupil shear) and IOS-IR-5799 (non-NIRCam pupil shear).

### 3.4 Pupil roll

Just like pupil shear, pupil roll is measured by comparing the OSIM PAR elements to the instrument PAR fiducials. In the case of NIRCam, PIL images are used in lieu of PAR images since the image quality from the NIRCam PARs is so poor. As one can see from Table 4 the final CV3 pupil roll values are almost all near or above the requirement of 10.6 mrad. In addition, just the 1-σ uncertainty the roll determination is near or above the requirement. These failures drove a significant effort into understanding the origin of the requirement and the functional limitations of the various pupil elements with respect to roll.

The original requirement, IOS-IR-5790, was written to guard against excessive pupil roll introducing vignetting of the OTE pupil by instrument imaging pupils. For non-imaging pupil elements like the DHS, the pupil roll requirement maintains registration of the OTE primary mirror segments with the subapertures in the DHS. Unfortunately, every type of pupil has its own functional limitation, and needs to be limited not simply in pupil roll but in a combination of shear and roll together.

The pupil types in the various SIs are:

MIRI Imager – Convoluted tricontagon, coronagraphic masks

NIRCam – Dodecagon, DHS, and Lyot masks

NIRISS – Tricontagon, Non-Redundant Mask (NRM)

NIRSpec – Oversized tricontagon

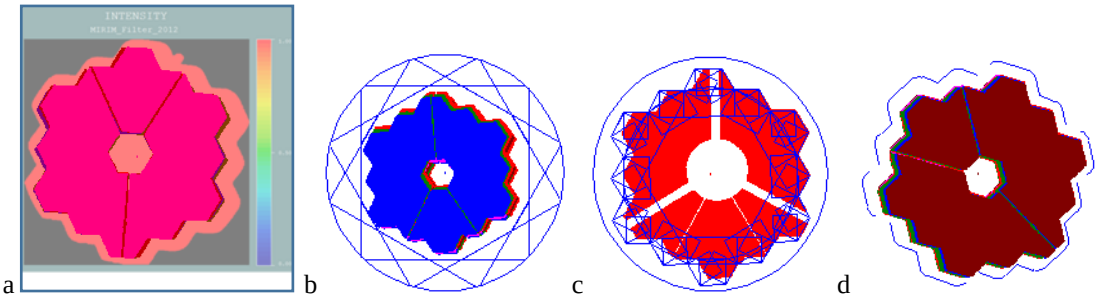


Figure 21. a) MIRI convoluted tricontagon. b) NIRCam dodecagon pupil. c) NIRISS tricontagon. d) NIRSpec oversized tricontagon.

The first pupil in each list is subject to a fairly simple consideration of vignetting for the measurement plus 2-σ equivalent pupil shear and roll from Table 4, and including contributions for the allocated OTE shear and roll in the opposite direction. The graphical results are shown in Figure 21 for the MIRI, NIRCam, NIRISS and NIRSpec. Only NIRISS was found to be at risk of vignetting with a maximum of 3% at the worst field point which was deemed acceptable by the NIRISS science team considering the probability of the occurrence. FGS does not have a physical stop at the pupil plane, but a similar ray tracing effort was performed to check for vignetting at baffles near the TMA3 mirror where the FGS PAR is located and none was seen. The effect on remaining pupils each have to be examined individually, below.

MIRI coronagraph

An internal study by the MIRI team examined the impact of pupil roll, field roll, and combinations of both (up to a maximum 1.0 degree pupil/field roll difference), on the coronagraphic rejection.[8] The worst case pupil roll from Table 4 is approximately 2 degrees in magnitude, while the worst-case radial pupil shear is 3.0% including the recently measured ISIM-OTE relative pupil shear. In order to estimate the effect for a 2-degree field-pupil difference we take the study's predicted value for perfectly aligned field and pupil at 3.0% shear of ~300 and subtract off twice the difference between that and the value for a 1-degree field-pupil error at 3.0% shear (predicted to be ~270), leaving an estimated rejection rate of 240. The requirements for coronagraphic rejection [MIR-0037, MIR-0038, MIR-0039, MIR-0040 as stated in JPL D-24158 - MIRI Functional Requirements Document] are that "The coronagraph shall provide a rejection factor of at least

30 (thirty) at [coronagraphy wavelength]." For even the worst case shear expected for both the instrument and the OTE, the performance of the MIRI coronagraphic mode is still expected to be approximately 8x better than the requirement.

NIRCam DHS

The NIRCam DHS subapertures are designed to capture light from only two adjacent OTE primary mirror segments in order to assist in the precise alignment of mirror segments with respect to one another. If light from a third adjacent segment is captured, then it can contaminate the signal and degrade the performance of the DHS mode. The OSIM Fine Phase Plate (FPP) mimics the physical apertures of each OTE primary mirror segment, with appropriate gaps between the segment apertures. Visual inspection of PIL images of the DHS and the OSIM FPP in Figure 22 show that there is no contamination from third segments. The original design specified that the DHS roll could not exceed 35 mrad (2 degrees).[9] While the worst-case pupil roll shown in Table 4 is worse than 2 degrees, these images demonstrate that the performance of the DHS is not impacted by the measured pupil shear and roll measured in CV3.

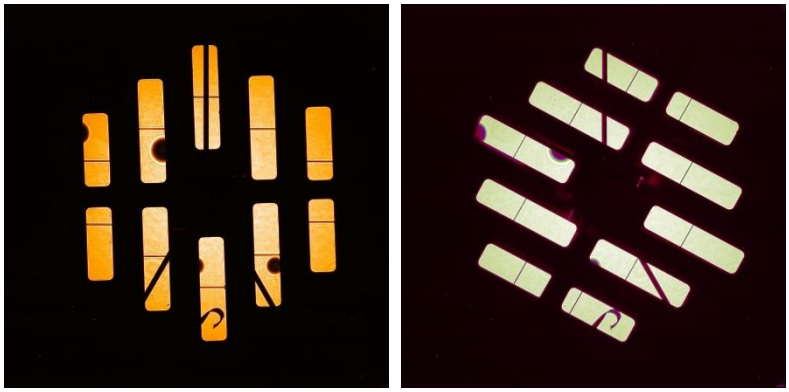

Figure 22. NIRCam PIL images of the OSIM FPP and the DHS0 (left) and DHS60 (right) elements in NIRCam A. No 3rd segment contamination is visible.

NIRCam Lyot stops

The other type of pupil stop in NIRCam are two Lyot stops used in combination with a coronagraphic mask located immediately downstream of the Fine Alignment Mirror (FAM), referred to as MASKBAR and MASKRND. PIL images of these two masks and the OSIM FPP are overlaid in Figure 23. The functional requirement is that no single aperture in each Lyot mask captures light from more than one OTE primary mirror segment. Again, visual inspection of the images shows that this is the case. One can see that the MASKRND apertures (the purple regions) do come quite close to the segment borders. This is largely due to the fact that the active field that these masks are used in is significantly different from the field point where the PIL can be used. This difference introduces a 0.5-0.7% pupil wander that shifts the MASKRND apertures with respect to the OTE pupil.

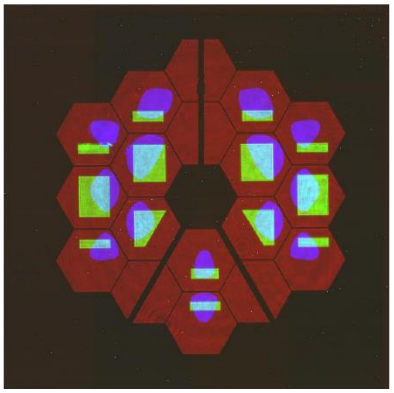

Figure 23. Overlaid PIL images of the NIRCam MASKBAR and MASKRND pupils and the OSIM FPP.

In addition to the visual evidence that mask apertures are contained within individual OTE segment boundaries, a sensitivity analysis was performed by members of the NIRCam team assuming the worst-case pupil roll measured for the DHS elements. John Krist reported that "there are very small differences in the morphology of the speckle patterns produced by the coronagraphic mask and Lyot stop combination, but no significant change in their overall brightnesses. This demonstrates that the observed misalignments do not have any significant impact on the NIRCam coronagraphic performance."[10]

NIRISS NRM

The NIRISS Non-Redundant Mask is similar in many ways to the NIRCam Lyot stops. The pupil element has a series of hexagonal apertures each of which captures light from a single OTE primary mirror segment. The footprint of light that each aperture sees shown in Figure 24. The closest approach of any footprint to an OTE mirror segment edge is the B6 element on the +V3 side which is 118 mm from the segment edge, equal to 1.79% pupil shear in the +V3 direction.[11]

The measured pupil shear and roll can cause the footprint to come closer to the mirror segment edge. The worst-case predicted on-orbit pupil shear in the +V3 direction for NIRISS and the OTE is 0.61% (-0.17% ± 0.78% 2-σ), or 40.2 mm

of the 118 mm margin. Additionally, we must account for the relative NIRISS/OTE pupil roll, which is 1.04 degrees (-0.164 ± 1.203 2-σ), or another 58.9 mm, for a total of 99.1 mm of the 118 mm margin.

In conclusion, while the ISIM CV2 and CV3 measurements of pupil roll do not meet the formal IOS requirement, the impacts of the violations have been deemed negligible to acceptable, considering the level of effort, cost schedule impact, and risk necessary to correct the violations. A waiver against the pupil roll requirement has been accepted at the Observatory level.

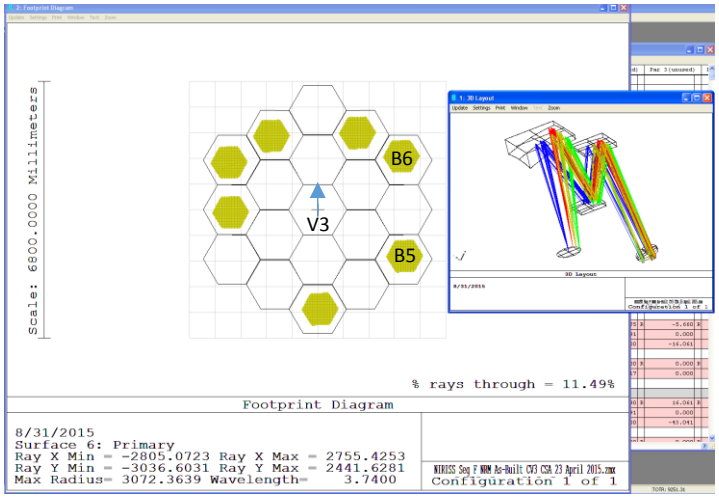


Figure 24. Footprint of light at the OTE that is captured by the apertures in the NIRISS NRM pupil mask. This figure and the initial technical baseline were provided by Anand Sivaramakrishnan of the Space Telescope Science Institute.

### 3.5 Boresight

The boresight for each instrument is defined as the chief ray angle at the center of the field-of-view for each instrument channel (FGS1, FGS2, MIRI Imager, NIRCam A SW, NIRCam A LW, NIRCam B SW, NIRCam B LW, NIRISS, and NIRSpec), with the "center" being defined as the average of the four corners of each channel's field-of-view. In calculating boresight, vignetting at the corners is ignored, and the field angle at the corner pixel positions is used.

In order to determine the field angle for each corner, some of which are vignetted, a combination of observation and modeling is used. First, in-focus images are taken near each corner or each field. The precise center of each PSF is found and that pixel position is correlated to the field angle defined by the OSIM pointing prescription[12]. The plate scale from the Code V optical model is then used to extrapolate the location of the nearby corner pixel. The center of field is calculated from the four corners, and the field angle at the center is compared to the boresight requirement, IOS-IR-5706, specifying a boresight error of less than 0.17 arcminutes (10.2 arcseconds) from the nominal optical model position in each axis.

The result of these calculations from ISIM CV3 are shown in Figure 25. The complete error budgets including uncertainties in boresight determination for each axis are shown in Table 6 and Table 7.

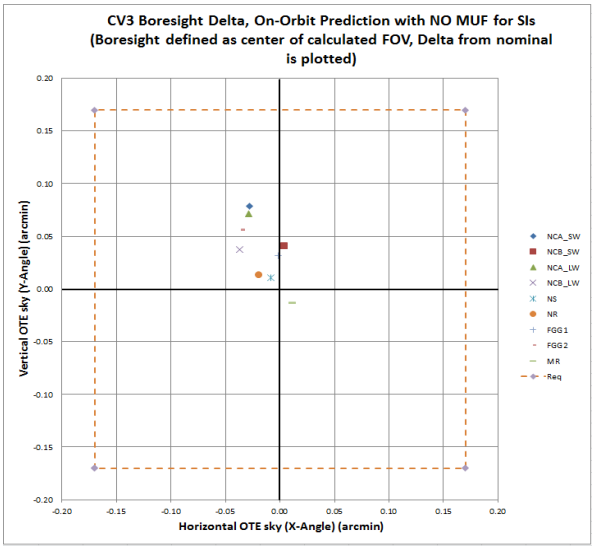


Figure 25. Boresight errors for all instrument channels, showing compliance with IOS-IR-5706. Value include the predicted shift for gravity and thermal differences between ground and on-orbit conditions. "MUF" refers to the Model Uncertainty Factor (1.4) that is not included in the values shown, but is included in the uncertainty values below.

| | | | | | | | | | | | | |
|---|---|---|---|---|---|---|---|---|---|---|---|---|
| | | | | ISIM Requirement | 10.20 | | | | | | | arcsec |
| | | | | Margin vs Requirement | 9.01 | 9.30 | 8.02 | 7.19 | 8.26 | 9.07 | | |
| | | | | | NIRSpec | MIRI | NIRISS | FGS | NIRCam A | NIRCam B | | |
| **Total Bottoms-up Estimate** | | | | | **1.19** | **0.90** | **2.18** | **3.01** | **1.94** | **1.13** | | |
| **Magnitude (best estimate of V2 boresight error)** | | | | | **0.60** | **0.78** | **1.26** | **2.04** | **1.68** | **0.90** | | |
| | Non-Common Path | | | | | | | | | | | |
| 1 | | CV3 measured boresight error | | | -0.60 | 0.78 | -1.26 | -2.04 | -1.68 | 0.90 | | |
| **Uncertainty (RSS of all terms below)** | | | | | **0.59** | **0.12** | **0.92** | **0.97** | **0.26** | **0.23** | | |
| 2 | | CV3 uncertainties | | | 0.07 | 0.07 | 0.85 | 0.91 | 0.07 | 0.07 | | |
| | | CV2-to-CV3 changes | | | 0.59 | 0.10 | 0.36 | 0.35 | 0.25 | 0.22 | | |

Table 6. Error budget for the V2 component of the boresight requirement IOS-IR-5706 showing compliance.

| | | | | | | | | | | | | |
|---|---|---|---|---|---|---|---|---|---|---|---|---|
| | | | | ISIM Requirement | 10.20 | | | | | | | arcsec |
| | | | | Margin vs Requirement | 8.65 | 9.10 | 6.53 | 3.36 | 4.70 | 7.60 | | |
| | | | | | NIRSpec | MIRI | NIRISS | FGS | NIRCam A | NIRCam B | | |
| **Total Bottoms-up Estimate** | | | | | **1.55** | **1.10** | **3.67** | **6.84** | **5.50** | **2.60** | | |
| **Magnitude (best estimate of V3 boresight error)** | | | | | **0.78** | **0.60** | **0.60** | **3.54** | **4.74** | **2.10** | | |
| | Non-Common Path | | | | | | | | | | | |
| 1 | | CV3 measured boresight error | | | 0.78 | -0.60 | 0.60 | 3.54 | 4.74 | 2.10 | | |
| **Uncertainty (RSS of all terms below)** | | | | | **0.77** | **0.50** | **3.07** | **3.30** | **0.76** | **0.50** | | |
| 2 | | CV3 uncertainties | | | 0.25 | 0.25 | 2.89 | 1.45 | 0.25 | 0.25 | | |
| | | CV2-to-CV3 changes | | | 0.73 | 0.43 | 1.05 | 2.97 | 0.72 | 0.43 | | |

Table 7. Error budget for the V3 component of the boresight requirement IOS-IR-5706 showing compliance.

## 4. CONCLUSIONS

The rigid body alignment of the ISIM Element and instruments contained therein has been characterized by ambient and cryogenic testing. The performance parameters associated with the 6 degree-of-freedom alignment of the ISIM Structure and instruments have been found to be compliant with requirements, with the exception of pupil roll. The impact of each pupil roll was carefully assessed based on the functional requirements of each type of pupil, and the performance has been deemed acceptable for all, despite the formal violation. A waiver against the pupil roll requirements has already been accepted by the Science Instrument teams and the Observatory.

## 5. ACKNOWLEDGEMENTS

The work presented in this paper is based on data taken during the ISIM CV test campaign, conducted at the NASA Goddard Space Flight Center (GSFC). We are indebted to the ISIM test personnel for test planning & execution, real-time data review, Science Instrument support, facilities maintenance, and overall support during the test. More generally, the collective effort and dedication of a much larger group of people made this work possible. The authors gratefully acknowledge the contributions of optical, mechanical, electrical, and systems engineers, managers, and scientists associated with the James Webb Space Telescope project as a whole, and the Integrated Science Instrument Module element, the Science Instruments within ISIM [namely the FGS Guider and NIRISS, provided by the Canadian Space Agency (CSA) and COM DEV; MIRI, provided by the European Consortium with the European Space Agency (ESA),

and by the NASA Jet Propulsion Laboratory (JPL); NIRCam, provided by the University of Arizona and Lockheed Martin; and NIRSpec, provided by ESA, with components provided by NASA GSFC], and the OSIM OGSE in specific. Broadly, JWST is led by NASA and we acknowledge the leadership from the JWST Project Office at GSFC and the valuable contributions from all NASA centers and Headquarters. JWST is also an international collaboration and we acknowledge the contributions of Science Instruments and personnel by CSA and ESA, along with their supporting contractors and partner universities.

We also gratefully acknowledge the valued leadership of Pamela Davila (GSFC, retired), Brent Bos (GSFC), and Phil Young (retired) in the earlier development of requirements, error budgets, and their organization.

This work is supported by the James Webb Space Telescope project at NASA Goddard Space Flight Center.

## 6. REFERENCES

[1] T. Hadjimichael, *et al.*, "Alignment of the James Webb Space Telescope Integrated Science Instrument Module element", Proc. SPIE 9951, 9951-11 (2016)
[2] J. Johnston, *et al.*, "Cryogenic thermal distortion performance characterization for the JWST ISIM structure", Proc. SPIE 8150, 815009 (2011)
[3] J. A. Sullivan, *et al.*, "JWST's optical telescope simulator for verification of the Integrated Science Instrument Module", Proc. SPIE 9951, 9951-13 (2016)
[4] R. Gracey, *et al.*, "Structural, thermal, and optical performance (STOP) modeling and results for the James Webb Space Telescope integrated science instrument module ", Proc. SPIE 9911, 99111A (2016)
[5] D. L. Aronstein, *et al.*, "Wavefront-error performance characterization for the James Webb Space Telescope (JWST) Integrated Science Instrument Module (ISIM) science instruments", Proc. SPIE. 9904, 9904-09 (2016)
[6] B. J. Bos, *et al.*, " Pupil alignment considerations for large, deployable space telescopes ", Proc. of SPIE Vol. 8131, 81310J (2011)
[7] D. A. Kubalak, *et al.*, "JWST science instrument pupil alignment measurements", Proc. SPIE 9951, 9951-12 (2016)
[8] A. Glasse, internal JWST communication
[9] S. Knight, internal JWST communication
[10] J. Krist, internal JWST communication
[11] A. Sivaramakrishnan, internal JWST communication
[12] D. Sabatke, *et al.*, "Ray-tracing for coordinate knowledge in the JWST Integrated Science Instrument Module", Proc. SPIE. 9293, 9293-06. (2014)